Final Results on the Measurement of the Structure Functions g_1^p and g_1^d at HERMES

Lara De Nardo[1,2]
on behalf of the HERMES Collaboration

1- DESY, 22603 Hamburg, Germany
2-TRIUMF, Vancouver, British Columbia V6T 2A3, Canada

Final results on precise measurements of the spin structure functions of the proton $g_1^p(x, Q^2)$ and deuteron $g_1^d(x, Q^2)$ are presented over the kinematic range $0.0041 \leq x \leq 0.9$ and 0.18 GeV$^2 \leq Q^2 \leq 20$ GeV^2. The data were collected at the HERMES experiment at DESY, in deep-inelastic scattering of 27.6 GeV longitudinally polarized positrons off longitudinally polarized hydrogen and deuterium gas targets internal to the HERA storage ring.

1 Introduction

The structure functions $g_1^{p,d}$ can be extracted from the measurement of double-spin asymmetries $A_{||}^{p,d}$ of cross sections in inclusive deep-inelastic scattering $\ell + N \to \ell + X$ of longitudinally polarized charged leptons off longitudinally polarized protons and deuterons:

$$g_1^{p,d}(x, Q^2) = \frac{1}{1 - \frac{y}{2} - \frac{y^2}{4}\gamma^2} \left[\frac{Q^4}{8\pi\alpha^2 y} \frac{\partial^2 \sigma_{UU}^{p,d}(x, Q^2)}{\partial x \partial Q^2} A_{||}^{p,d}(x, Q^2) + \frac{y}{2}\gamma^2 \, g_2^{p,d}(x, Q^2) \right] , \qquad (1)$$

when a model is used for the unpolarized cross section $\partial^2 \sigma_{UU}^{p,d}(x, Q^2)/\partial x \partial Q^2$ and the structure function $g_2^{p,d}$ In Eq. (1) x is the fraction of the nucleon's light-cone momentum carried by the struck quark, $-Q^2$ is the squared four-momentum transferred by the virtual photon, and y and γ are kinematic factors.

At any order in $\alpha_s(Q^2)$ and in a leading-twist approximation, the proton and neutron structure functions $g_1^{p,n}$ are a convolution of singlet ($\Delta\Sigma(x, Q^2)$), non-singlet ($\Delta q_{NS}^{p,n}(x, Q^2)$) and gluon helicity distributions ($\Delta g(x, Q^2)$) [2] with the corresponding Wilson coefficient functions $\Delta C(x, \alpha_s(Q^2))$ [3]:

$$g_1^{p,n}(x, Q^2) = \frac{1}{2}\langle e^2 \rangle \left[\Delta C_\Sigma \otimes \Delta\Sigma + 2N_q \Delta C_g \otimes \Delta g + \Delta C_{NS}^{p,n} \otimes \Delta q_{NS}^{p,n} \right] . \qquad (2)$$

The deuteron structure function g_1^d is related to g_1^p and g_1^n by the relation:

$$g_1^d = \frac{1}{2}(g_1^p + g_1^n)\left(1 - \frac{3}{2}\omega_D\right) , \qquad (3)$$

where $\omega_D = 0.05 \pm 0.01$ takes into account the D-state admixture to the deuteron wave function. The last expression allows for the extraction of the neutron structure function g_1^n from the combined measurements of g_1^p and g_1^d at the same values of x and Q^2.

These proceedings report on the final results on the HERMES measurement of the structure functions g_1^p and g_1^d, with the consequent extraction of g_1^n. Details can be found in Ref. [4].

2 Data

Proton data were collected in 1996 and 1997 (the latter have been previously published in [5]), while the deuteron data were collected in the year 2000. While the accuracy of the HERMES proton data is comparable to that of earlier measurements, the HERMES deuteron data are more precise than all published data.

Kinematic and geometric cuts were imposed to make sure that the event was a DIS event and that the lepton tracks were fully contained within the spectrometer aperture, which limits the acceptance to scattering angles $0.04 \leq \theta \leq 0.22$ mrad. The constraint $y > 0.1$ excludes regions of low momentum resolution [6], $y \leq 0.91$ discards the low momentum region where the trigger efficiencies have not yet reached a momentum plateau. The requirement $W^2 > 3.24$ GeV^2 suppresses the region of baryon resonances. The resulting (x, Q^2) region, defined by $0.0041 \leq x \leq 0.9$ and 0.18 GeV$^2 \leq Q^2 \leq 20$ GeV^2, was divided into 19 bins in x and into up to 3 bins in Q^2, guided by the available statistics. The positron and electron identification was achieved with a probability analysis based on the responses of the Transition Radiation Detector, the Pre-Shower Detector, the Calorimeter, and the Čerenkov Detector (for proton data) or the RICH Detector (for deuteron data). A correction for charge symmetric background from meson Dalitz decays or photon conversions into e^+e^- pairs was applied in each kinematic bin by subtracting the number of leptons with the charge opposite to that of the beam particle. Such a correction reaches up to 25% and is concentrated in the high-y bins.

3 Extraction

The measured asymmetry $A_{||}^m$ was obtained from the number of events obtained when the polarization of the lepton beam and that of the target nucleons were parallel ($N^{\rightrightarrows}$) and anti-parallel ($N^{\rightleftarrows}$) as:

$$A_{||}^m(x, Q^2) = \frac{1}{P_T P_B} \frac{N^{\rightleftarrows}(x, Q^2)\ \mathcal{L}^{\rightrightarrows} - N^{\rightrightarrows}(x, Q^2)\ \mathcal{L}^{\rightleftarrows}}{N^{\rightleftarrows}(x, Q^2)\ \mathcal{L}^{\rightrightarrows} + N^{\rightrightarrows}(x, Q^2)\ \mathcal{L}^{\rightleftarrows}} \tag{4}$$

where $\mathcal{L}^{\rightrightarrows}$ and $\mathcal{L}^{\rightleftarrows}$ are the deadtime-weighted luminosities, while P_B ($P_B = 0.53 \pm 0.018$ for proton and $P_B = 0.53 \pm 0.010$ for deuteron data) and P_T ($P_T = 0.85 \pm 0.032$ for proton and $P_T = 0.84 \pm 0.03$ for deuteron data) are the beam and target average polarizations. After data selection as discussed above, the events available for asymmetry analyses on proton and deuteron were 3.5M for the proton and 10.2M for the deuteron.

The asymmetry $A_{||}$ was evaluated separately for the top and bottom halves, thus allowing polarization-independent systematic effects present in each detector half to cancel independently, and the final asymmetry was obtained as the weighted average of the two. In the case of the deuteron the measured asymmetry was corrected for the small contribution coming from the tensor structure function b_1^d, previously measured at HERMES [7]. Corrections for radiative and detector smearing effects, as well as for the background coming from elastic and quasi-elastic scattering were achieved with the application of an unfolding algorithm. After unfolding, the data points are statistically correlated but systematic correlations due to kinematic smearing have been removed, resulting in a resolution of a single-bin width.

The structure function g_1^p and g_1^d were then extracted from the Born asymmetry using the parameterizations [8], [9] and [10] to model the unpolarized cross section, while g_2 was

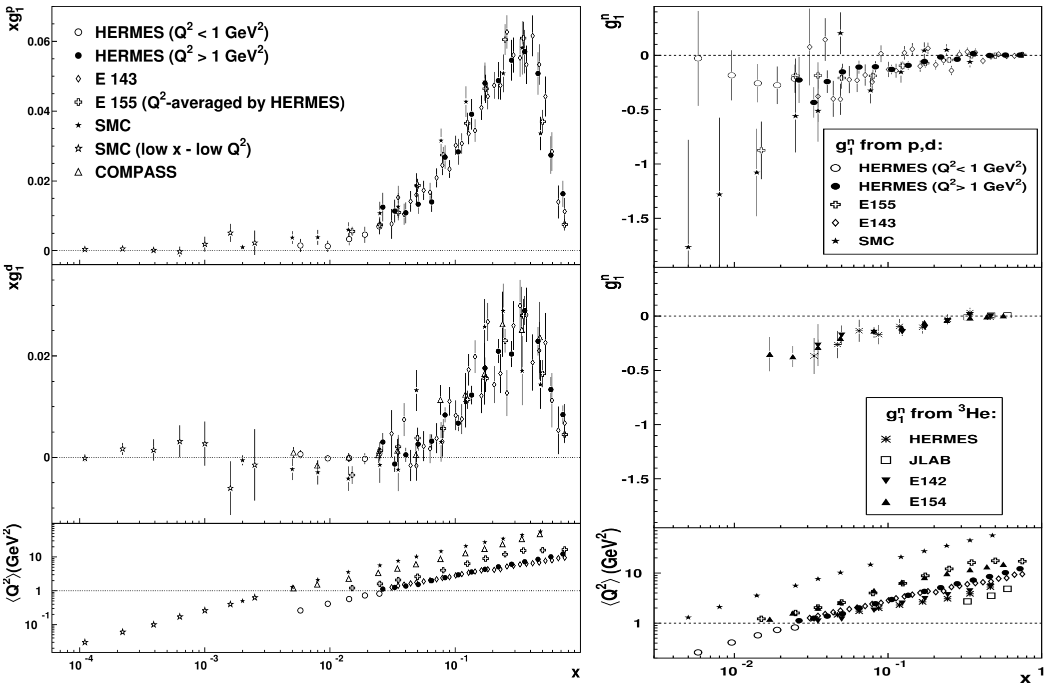

Figure 1: Left panel: HERMES results on xg_1^p and xg_1^d vs x, shown on separate panels, compared to data from SMC [11], E143 [12], E155 [13], and COMPASS [14]. The HERMES data points are statistically correlated by unfolding QED radiative and detector smearing effects. Right panel, top plot: the structure function g_1^n obtained from g_1^p and g_1^d, compared with similar data from SMC [11], E143 [12], and E155 [13] in the HERMES x-range. Right panel, second plot from the top: g_1^n as obtained from an ^{3}He target [21]. The bottom panels show the $\langle Q^2 \rangle$ of each data point in the top two panels. In all plots the error bars represent total uncertainties.

computed from a parameterization of all available proton and deuteron data [15, 16, 17, 18, 19]. The values of g_1 at the average Q^2 in each x bin were obtained from the evolution of the g_1 values in each Q^2 bin to the average Q^2 in each x bin by using an NLO QCD fit to all available g_1 data based on the 'BB' code [20], The systematic uncertainties originate from the experiment (beam and target polarizations, particle identification, misalignment of the detector) and the parameterizations (g_2, F_2, R, A_{zz}^d, ω_D), with the largest contributions coming from the beam and target polarization uncertainties.

The results are shown in Fig.1 (left), in comparison with those from other experiments. In the case of the proton, the central values of the SMC data points are larger than those of HERMES, in the low-x region. This reflects the difference in $\langle Q^2 \rangle$ values between the two experiments, and is expected from the Q^2 evolution of g_1. In the case of the deuteron, the HERMES data are compatible with zero for $x < 0.04$. In this region the SMC data favor negative values for g_1^d while the COMPASS results [14], at a similar Q^2 of SMC, are also consistent with zero.

The neutron structure function g_1^n was extracted from g_1^p and g_1^d using Eq. (3) and is shown in the right panel of Fig. 1. Compared to previous data, $g_1^n(x)$ is now very well restricted by the HERMES measurement. The structure function g_1^n is slightly positive in the very high x region, and negative everywhere else. The new results suggest that g_1^n gradually approaches zero from below and, while it is based on data with $Q^2 \leq 1$ GeV^2, it does not support the earlier conjecture of a strong decrease of $g_1^n(x)$ for $x \to 0$ based on the E154 and SMC data.

The first moments of g_1 provide important information on the spin structure of the nucleon, in particular when results on proton, deuteron and neutron are combined. The precision of the integrals is less affected by the unfolding procedure since all inter-bin correlations from the unfolding procedure are taken into account. For $x < 0.04$, $g_1^d(x)$ becomes compatible with zero and its measured integral shows saturation. Under this assumption, and assuming of the validity of SU(3) flavor symmetry in hyperon β-decays, the values $\Delta s + \Delta\bar{s} = -0.085 \pm 0.013(\text{theo.}) \pm 0.008(\text{exp.}) \pm 0.009(\text{evol.})$ (negative and different from zero by about 4.7 σ), $\Delta u + \Delta\bar{u} = 0.842 \pm 0.004(\text{theo.}) \pm 0.008(\text{exp.}) \pm 0.009(\text{evol.})$ and $\Delta d + \Delta\bar{d} = -0.427 \pm 0.004(\text{theo.}) \pm 0.008(\text{exp.}) \pm 0.009(\text{evol.})$ are obtained for the quark distributions, using HERMES deuteron data alone, in the $\overline{MS}$ scheme at order $\mathcal{O}(\alpha_s^2)$, at $Q^2 = 5$ GeV^2. Additionally, the total quark contribution to the nucleon's spin is obtained as $\Delta\Sigma = 0.330 \pm 0.011(\text{theo.}) \pm 0.025(\text{exp.}) \pm 0.028(\text{evol.})$. This result suggests that the nucleon helicity gets a substantial contribution from quark helicities, even though there is still need for contributions from gluon helicities and angular momentum.

References

[1] Slides:
`http://indico.cern.ch/contributionDisplay.py?contribId=135&sessionId=4&confId=9499`

[2] G. Altarelli *et al.*, Nucl. Phys. **B496** 337 (1997).

[3] R. Mertig and W.L. van Neerven, Z. Phys. **C70** 637 (1996).

[4] A. Airapetian *et al.*, Phys. Rev. **D75** 0122007 (2007).

[5] A. Airapetian*et al.*, Phys. Lett. **B442** 484 (1998).

[6] K. Ackerstaff *et al.*, Nucl. Instrum. Meth. **417** 230 (1998).

[7] A. Airapetian *et al.*, Phys. Rev. Lett. **95** 242001 (2005).

[8] H. Abramowicz and A. Levy, arXiv:hep-ph/9712415 (1997).

[9] P. Amaudruz *et al.*, Nucl. Phys. **B371** 3 (1992).

[10] L.W. Whitlow *et al.*, Phys. Lett. **BB250** 193 (1990).

[11] B. Adeva *et al.*, Phys. Rev. **D58** 112001 (1998); B. Adeva *et al.*, Phys. Rev. **D60** 072004 (1999); B. Adeva *et al.*, Phys. Rev. **D62** 079902 (2000).

[12] K. Abe *et al.*, Phys. Rev. **D58** 112003 (1998).

[13] P.L. Anthony *et al.*, Phys. Lett. **B493** 19 (2000); P.L. Anthony *et al.*, Phys. Lett. **B463** 339 (1999).

[14] E.S. Ageev *et al.*, Phys. Lett. **B612** 154 (2005).

[15] P.L. Anthony *et al.*, Phys. Lett. **B458** 529 (1999).

[16] K. Abe *et al.*, Phys. Rev. Lett. **76** 587 (1996).

[17] P.L. Anthony *et al.*, Phys. Lett. **B553** 18 (2003).

[18] D. Adams *et al.*, Phys. Lett. **B336** 125 (1994).

[19] D. Adams *et al.*, Phys. Lett. **B396** 338 (1997).

[20] J. Blümlein and H. Böttcher, Nucl. Phys. **B 636** 225 (2002).

[21] X. Zheng *et al.*, Phys. Rev. **C70** 065207 (2004); K. Ackerstaff *et al.*, Phys. Lett. **B404** 383 (1997); P.L. Anthony *et al.*, Phys. Rev. **D54** 6620 (1996); K. Abe *et al.*, Phys. Rev. Lett. **79** 26 (1997).